JOURNAL OF AGRICULTURAL AND FOOD CHEMISTRY

J. Agric. Food Chem. **2006,** *54,* 9677−9686 **9677**

Differences between Lignin in Unprocessed Wood, Milled Wood, Mutant Wood, and Extracted Lignin Detected by ^{13}C Solid-State NMR

JINGDONG MAO,[†] KEVIN M. HOLTMAN,[‡] JAY T. SCOTT,[§] JOHN F. KADLA,[#] AND KLAUS SCHMIDT-ROHR*,[†]

Department of Chemistry, Iowa State University, Ames, Iowa 50011; PWA, WRRC, BCE, Agricultural Research Service, U.S. Department of Agriculture, 800 Buchanan Street, Albany, California 94710; Department of Wood and Paper Science, North Carolina State University, Raleigh, North Carolina 27695; and University of British Columbia, 4034-2424 Main Mall, Vancouver, British Columbia V6T 1Z4, Canada

Solid-state ^{13}C nuclear magnetic resonance (NMR) spectroscopy was applied to intact and isolated loblolly pine wood samples to identify potential structural changes induced by tree age, milling, lignin extraction, or naturally occurring mutations. Special attention was paid to ketone and aldehyde as well as nonpolar alkyl groups, which could be observed at low concentrations (<2 in 1000 C) using improved spinning-sideband suppression with gated decoupling. Carbonyl structures were present in intact wood, and there are more keto groups than aldehydes. Their concentrations increased from juvenile to mature wood and with milling time, whereas extraction did not alter the C═O fraction. Significant amounts of aldehyde and dihydroconiferyl alcohol residues were present in coniferyl aldehyde dehydrogenase-deficient wood, confirming solution-state NMR spectra of the corresponding lignin. These results demonstrate the utility of solid-state NMR as an assay for changes in the lignin structure of genetically modified plants.

KEYWORDS: Lignin; lignin in wood; lignin isolation; milled wood lignin (MWL); solid-state NMR; spectral editing

INTRODUCTION

Native lignin is an amorphous, three-dimensional copolymer of phenylpropanoid units linked through ether and carbon−carbon bonds. It provides mechanical support for plants, as well as facilitating transport of nutrients and providing defense against attack from microorganisms (*1*−*5*). Polymerization of monolignols occurs within the cell wall, embedded in a polysaccharide gel, thereby producing molecular association and possibly covalent linkages of lignin and polysaccharides (*4*, *6*, *7*). Due to this intimate association, quantitative isolation of the complete lignin polymer has proven to be impossible. As a result, most structural information has come from isolated lignin preparations, specifically solution-state nuclear magnetic resonance (NMR) of milled wood lignin (MWL) (*8*−*19*), which is typically only 15−20% of the native lignin and is extracted as a dioxane-soluble, low molecular weight material (*20*).

It is known that the structure of lignin is modified by the commonly used milling processes and solvent extraction techniques (*21*), although the extent of structural changes has not been verified. As a result, relatively minor structural features may be merely artifacts of lignin isolation. Additionally, there have been many reports on the heterogeneous nature of lignin in wood, and it has been shown that the layers of the cell walls are not proportionally represented in the MWL (*22*−*24*). As a result, it would be preferable to analyze the structure of lignin intact in wood.

Solid-state NMR can address the issue of processing-induced structural changes or selective extraction, because it can provide spectra of whole wood as well as lignin. However, previous solid-state NMR studies of wood and lignin have mostly focused on the three major substitution types of the aromatic rings in lignin (*9*, *25*, *26*) rather than on differences between lignin before and after separation from other components of wood. The bonding structures of the three-carbon alkyl components in the lignin repeat units have been rarely investigated in native plants, requiring ^{13}C labeling and difference spectroscopy to remove the overlap with cellulose resonances (*27*, *28*).

Discrimination between true and processing-induced structures is particularly relevant in the evaluation of the effects of transgenics and natural mutations. In this study, we applied solid-state NMR to probe potential structural changes induced by the milling of wood and to quantify the levels of coniferyl

* Corresponding author [telephone (515) 294-6105; fax (515) 294-0105; e-mail srohr@iastate.edu].
[†] Iowa State University.
[‡] U.S. Department of Agriculture.
[§] North Carolina State University.
[#] University of British Columbia.

10.1021/jf062199q CCC: $33.50
Published on Web 12/10/2006

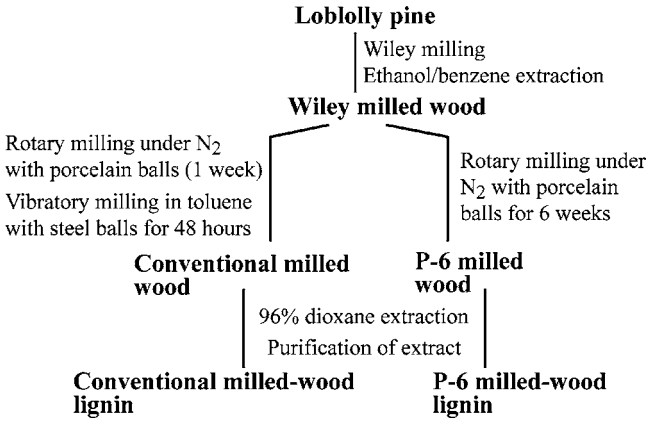

Figure 1. Procedure for the different milling techniques and the milled wood lignin (MWL) isolation.

aldehyde and dihydroconiferyl alcohol in intact coniferyl aldehyde dehydrogenase (CAD)-deficient loblolly pine by ^{13}C solid-state NMR. A combination of total suppression of spinning sidebands (TOSS) with an improved dipolar dephasing scheme was used, which prevents dipolar dephasing from reintroducing sidebands. Additionally, pulse sequences novel to wood chemistry are applied to separate methine and methylene carbons from overlapping peaks. Such experiments can be used to provide assay capabilities to scan sets of genetically modified plants for structural changes without the arduous task of lignin isolation. Most significantly, we can investigate the lignin component in intact woods, which cannot be achieved using solution NMR.

MATERIALS AND METHODS

Samples. Wood samples used in this study were of two different origins: mature loblolly pine (*Pinus taeda*) and a pair of samples from juvenile (4-year-old) loblolly pines, one expressing a natural mutation exhibiting a 99% deficiency in the cinnamyl alcohol dehydrogenase enzyme responsible for reducing coniferyl aldehyde to coniferyl alcohol (CAD-nl) and the other a wild type for reference.

The mature loblolly pine was analyzed as the intact wood sample and after having been ground to pass a 20-mesh screen and Soxhlet extracted with ethanol/benzene and ethanol for 24 h each (Wiley milled wood). The Wiley milled wood was further milled by two different techniques to produce two distinct wood flours. The first batch was milled according to our standard technique, 1 week of rotary milling under a N_2 atmosphere with porcelain balls, followed by 2 days of vibratory milling in toluene with steel balls [conventionally milled wood, termed "Vibratory in Toluene Wood" in previous work (*18*)]. The second technique involves 6 weeks of milling in the rotary ball mill under a N_2 atmosphere with porcelain balls [P-6 milled wood, termed "Rotary Porcelain 6 Week Wood" in previous work (*18*)]. From each of these wood flours, the MWL was isolated in the typical manner (*21*) (**Figure 1**).

NMR Spectroscopy. *Experimental Parameters.* The experiments were performed in a Bruker DSX400 spectrometer at 100 MHz for ^{13}C with 7-mm rotors and in a double-resonance probe. Intact, cylindrical wood pieces of sizes fitting 7-mm rotors were cut from the outermost growth ring(s) of the wood samples. ^{13}C CP/TOSS (cross polarization/total sideband suppression) experiments at a spinning speed of 6.5 kHz and a CP time of 1 ms, with a ^1H 90° pulse length of 4 μs, were run. The recycle delay was 1 s in order to optimize sensitivity in a given measuring time. We checked that the shape of the 1-s spectrum of milled wood lignin (MWL) was identical to that of the fully relaxed 3-s spectrum. This is expected due to efficient spin diffusion between protons on a 50-nm scale within 1 s, which makes their longitudinal relaxation times identical. Numbers of scans ranged between 40K and 104K for wood samples and between 10K and 40K for lignin samples. For optimized detection of aldehyde ^{13}C resonances, irradiation of the

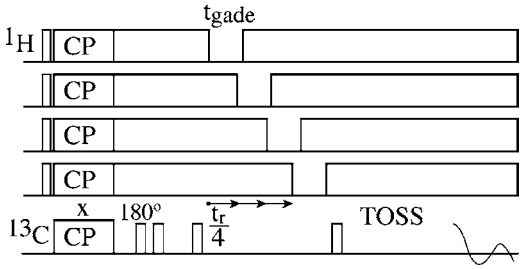

Figure 2. Pulse sequence of the improved dipolar dephasing technique with total suppression of sidebands (TOSS). The four different timings of the gated decoupling shown are run in a loop after completion of the TOSS phase cycle.

^{13}C pulses was at 160 ppm and decoupling of ^1H at 9 ppm for most spectra shown. The measuring time for 16 spectra together was 130 h. For optimized detection of signals in the alkyl-C region of the native and homozygous CAD-deficient wood, irradiation of ^{13}C was applied at 80 ppm and decoupling of ^1H at 2.5 ppm; for either spectrum, 36K scans were averaged (20-h total measuring time).

Spectral editing was also applied. CH-only spectra were obtained by dipolar DEPT (*29*) at a 5.787-kHz spinning speed. To remove the OCH_3 signal completely, the dipolar dephased spectrum (*29*) in the alkyl-C region was scaled up by 1.6 before taking the difference. Sixty thousand scans total were averaged. Spectral editing of immobile CH_2 signals by three-spin coherence selection (*30*) was applied at a spinning speed of 5.787 kHz. In addition to a CH_2OH band near 63 ppm, signals of ethers ($C-O-CH_2-C$) at 72 ppm and of nonpolar CH_2 groups ($C-CH_2-C$) at 40 ppm can be seen. One hundred and twelve thousand scans were averaged. Selection of immobile sp^3-hybridized CH_2 and CH carbons (*31*) was achieved by a 70-μs CSA filter [three-pulse version (*31*)] combined with short, 50-μs CP, at 5-kHz MAS; 16K scans were averaged. Selection of immobile $-CH$ and $-CH_2$ signals was achieved by short-CP minus short-CP plus dipolar dephasing (*32*) at 6.5-kHz MAS, with 64K scans total. Some residual signal of the dominant OCH_3 peak is observed in many of these spectra. The pulse programs for these experiments can be found at http://www.public.iastate.edu/~nmrksr.

Improved Dipolar Dephasing with Sideband Suppression. Dipolar dephasing, that is, gating the decoupler off for ~40 μs, is a simple but useful spectral-editing method for generating a subspectrum of nonprotonated carbons and mobile groups, such as rotating CH_3 (*33*). However, the orientation dependence of the C−H dipolar coupling (*34*) results in differential dephasing that interferes with sideband suppression by TOSS. TOSS requires equal contributions from carbons at various orientations, traditionally characterized by the angle γ (*34*). The residual sideband of protonated aromatic carbons observed near 200 ppm at spinning frequencies near 7 kHz is particularly troublesome for spectroscopy of keto and aldehyde groups, which resonate in this spectral range. Significantly faster spinning would require smaller rotors, which take less sample and therefore reduce the sensitivity by >2-fold, which is problematic for detection of small C═O signals.

To eliminate the residual sidebands, 40-μs dipolar dephasing was combined with an incrementation of its position in the rotation period in four steps of ~t_r/4 within the TOSS pulse sequence, as shown in **Figure 2**. This provides the "γ-integral" that suppresses sidebands up to fourth order (*35*). In other words, signals of the same C−H carbon are superimposed with various C−H dephasing factors that average out and permit TOSS to work correctly.

RESULTS AND DISCUSSION

Overview Spectra. Figure 3 gives examples of the ^{13}C NMR (CP/TOSS) spectra of the intact pieces of three loblolly pines: mature wood (**Figure 3A**), 4-year-old juvenile wood (**Figure 3B**), and 4-year-old juvenile mutant wood (**Figure 3C**). In addition, panels **D**−**F** of **Figure 3** show spectra of variously milled wood samples. Because cellulose and hemicellulose comprise approximately 70% of the dry weight of wood, the

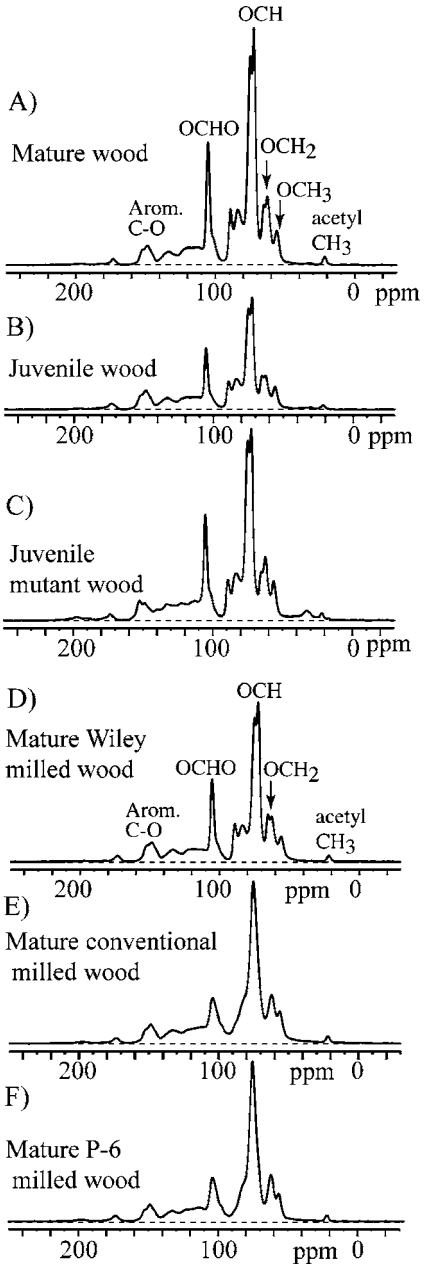

Figure 3. Solid-state CP/TOSS ^{13}C NMR spectra of (**A**) mature wood, (**B**) juvenile wood (wild type), (**C**) juvenile mutant wood (homozygous CAD-deficient wood), (**D**) mature Wiley milled wood, (**E**) mature conventionally milled wood, and (**F**) mature P-6 milled wood, all from loblolly pines. The spectra have been scaled to equal height of the lignin peak at 148 ppm.

spectra are dominated by carbohydrate resonances between 108 and 60 ppm. After intense milling, these peaks have broadened greatly (**Figure 3E**,**F**), which was observed previously and is attributed to the destruction of the crystalline structure of the cellulose.

Aromatic Moieties. Figure 4 presents ^{13}C NMR spectra of variously processed samples, demonstrating the effects of different milling techniques and lignin extractions on the aromatic portion of the lignin. The ^{13}C CP/TOSS spectra in the left column show all of the qualitative information on each sample; they have been scaled to make the aromatic peaks of the lignin component well visible even in the whole-wood samples. Those in the right column, that is, dipolar-dephased spectra obtained with the pulse sequence of **Figure 2**, display signals of nonprotonated carbons and of mobile segments, in particular, rotating methyl groups. Residual signals of the large OCH peaks of cellulose are most likely due to partly mobile carbohydrate residues. The corresponding spectra of juvenile whole wood (wild type) and a juvenile mutant wood are shown in **Figure 5**.

Features in the wood spectra that are exclusively associated with lignin include not only the downfield aromatic and C═O resonances but also the methoxyl peak of the guaiacyl lignin at 56 ppm. The acetyl-CH_3 band of the hemicelluloses is observed at 21.6 ppm, whereas the acetyl C═O contributes significantly to the peak at 172 ppm (*36*). Some further signal assignment is provided by dipolar dephasing, using the improved pulse sequence of **Figure 2**, which suppresses the signals of rigid protonated carbons by introducing a 40-μs period of gated decoupling. For instance, the dipolar dephasing of a significant fraction of the resonances near 200 ppm identifies these signals as arising from aldehydes, HC═O. To measure the small C═O signals around 196 ppm without reduction by excitation effects, we placed the carrier frequency at 160 ppm for ^{13}C.

Due to the limited overlap of cellulose and aromatic lignin peaks, we can compare the aromatic components of all samples, including the untreated and the milled wood. This allowed us to detect potential structural modifications by changes in the peak patterns of the aromatic fraction due to milling or extraction. The aromatic carbon spectra for mature and juvenile whole wood, **Figures 4A** and **5A**, respectively, matched very closely. The aromatic C−O peak near 148 ppm appeared to be slightly reduced, relative to the shoulder at 152 ppm, which tracked the rest of the aromatic signal more closely, after intensive milling and in the extracted lignins. By comparison, the spectra of mutant wood displayed in panels **C** and **D** of **Figure 5** showed major differences in peak intensities. Processing-induced changes in the C═O peak near 195 ppm will be discussed below.

The comparison can be made more quantitative by comparing the integral of the aromatic C−O region (162−142 ppm) with that of the total aromatic resonances. In the whole wood, the cellulose O−CH−O signal prevented integration to chemical shifts below 109 ppm, but analysis of the extracted-lignin spectrum shows that the aromatic signal extending to <109 ppm accounts for only 4.5% of all aromatic C. We corrected the 162−109 ppm whole-wood aromatic integrals correspondingly. Although cross polarization does not produce completely quantitative results, in the present samples the signal distortions are minor. In the lignin structures of **Figure 7**, all carbons are within one or two bonds from the nearest proton, and at the moderate spinning frequency used, the two-bond transfer is >90% complete within the 1-ms cross-polarization time.

Table 1 shows the number of C−O carbons per aromatic ring. The observed values were near 2, as expected for guaiacyl lignin with its two etherified carbons (C_3 and C_4). The specific values for the two MWL samples were very similar to those found in solution NMR (~5% smaller) (*18*). Significantly lower values, between 1.62 and 1.74, were found for the three whole-wood samples. The aromatic C−O concentration increased significantly in the Wiley milled wood, probably due to the removal of extractives and low molecular weight materials by Soxhlet extraction. Comparison of panels **A** and **C** of **Figure 4** showed a reduction of bands in the 125−100 ppm region, which corresponds to aromatic and olefinic C−H moieties commonly found in extractive compounds. Although the extracted compounds appeared to represent 15% of the sp^2-hybridized carbons, they accounted for only $\sim 0.3 \times 15\% = 5\%$ of all carbons, because lignin makes up only 30% of the sample. This agreed with an extractive content of around 5% found in an earlier

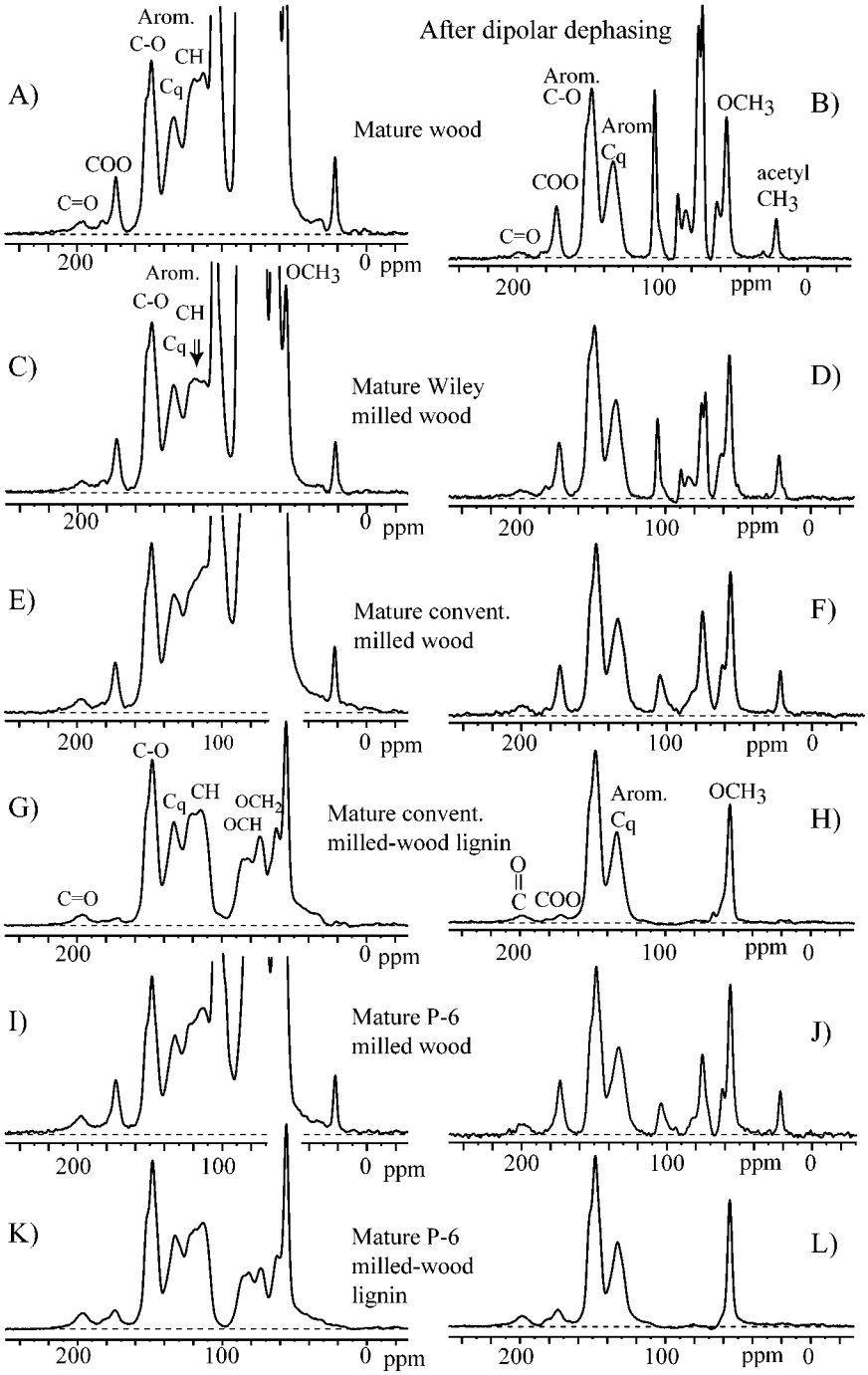

Figure 4. Solid-state CP/TOSS ^{13}C NMR spectra (left column) and corresponding dipolar dephased spectra, showing signals of nonprotonated (quaternary, "C_q") and of methyl carbons (right column) of (**A**, **B**) mature wood, (**C**, **D**) mature Wiley milled wood, (**E**, **F**) mature conventional MWL, (**G**, **H**) mature conventional MWL (**I**, **J**) mature P-6 milled wood, and (**K**, **L**) mature P-6 MWL, all from loblolly pines.

study (*37*). Reductions in the alkyl C signals from extractives were obscured by the overwhelming intensity of the carbohydrate peaks. The intensity of the OCH_3 signals, which can be observed free of overlap in the dipolar-dephased spectra, tracked quite closely with the aromatic C−O signal, as expected. The only exception was the larger OCH_3 resonance observed in the CAD-deficient sample, which highlights the pronounced structural changes due to the mutation.

Ketone and Aldehyde Quantification. Figure 6 focuses on the lignin signals in the downfield region. The smallest peaks correspond to ca. 2 in 1000 carbons. For a meaningful comparison, the aromatic C−O signals in all of the spectra were scaled to equal area. Dipolar dephasing identified aldehydes (H−C═O), which are the only protonated carbons that resonate downfield of 170 ppm in diamagnetic materials. The nonprotonated carbonyls of ketones and quinones in this same range were not significantly reduced by dipolar dephasing, and thus the amounts of aldehydes could be quantified by difference.

To make the comparisons more quantitative, we obtained the ratio of the integral between 220 and 187 ppm relative to the integral between 163 and 142 ppm (aromatic ethers and phenols) for each sample. The integral between 220 and 187 ppm from the ^{13}C CP/TOSS spectrum was that of all C═O carbons (aldehyde and keto groups; quinones are unlikely to occur in appreciable amounts in these samples). The integral between 220 and 187 ppm from the ^{13}C CP/TOSS spectrum after dipolar dephasing was that of nonprotonated C═O (keto groups). The difference was due to H−C═O carbons (aldehydes). The C═

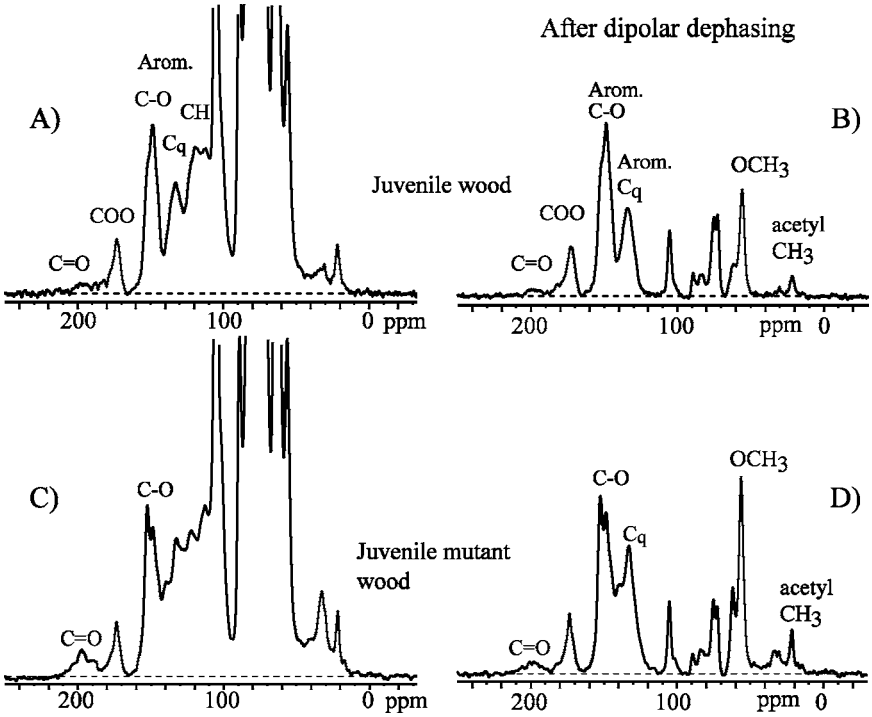

Figure 5. Solid-state CP/TOSS ^{13}C NMR spectra (left column) and corresponding dipolar dephased spectra of (**A**, **B**) juvenile wood and (**C**, **D**) juvenile mutant wood.

Table 1. Estimated Number of Aromatic C–O Carbons per Aromatic Ring[a]

	mature wood	Wiley milled wood	conventionally milled wood	MWL (conventional)	P-6 milled wood	P-6 MWL	juvenile wood	CAD-nl wood
C–O/ring	1.68	1.98	1.77	1.92	1.86	2.04	1.74	1.62

[a] The systematic error due to differences in chemical-shift anisotropy and cross-polarization efficiency is ~ ±10%, but the relative uncertainty, when different values in the table are compared, is smaller (~ ±5%), because all samples are subject to similar systematic errors.

O peaks were integrated relative to the aromatic C—O region (163−142 ppm). This gave the number of C═O per aromatic C—O, after multiplication by a factor of 0.85 to correct for the higher detection efficiency of C═O compared to aromatic carbons in TOSS. For each sample, the number of C═O per aromatic C—O was converted to the number of C═O per aromatic ring by multiplication with the number of aromatic C—O per aromatic ring, that is, with the factor given in **Table 1**. The results are listed in **Table 2**.

The C═O numbers per ring found in the two lignins were ~1.6 times larger than reported in a solution-state NMR study of the same samples (*18*). This deviation is larger than the uncertainty of the solid-state NMR values (±20%). It cannot be attributed to insufficient cross polarization of nonprotonated carbons, because fewer C═O than aromatic carbons are protonated, which means that C═O carbons should be underestimated rather than overestimated. It may be partly due to excitation effects in high-field solution ^{13}C NMR. With a 10-μs 90° pulse, the excitation profile decreases by about 15% for sites that are 12 kHz off-resonance (*34*). With excitation near the middle of the spectrum (at ~100 ppm) and given 125 Hz/ppm (*18*), the C═O peaks at 195 ppm are indeed about 12 kHz off-resonance. Limited probe-head bandwidth may have further reduced the detection efficiency in solution NMR. To minimize excitation effects, the solid-state NMR experiments were performed with irradiation near the C═O peaks (35 ppm off resonance) with strong, short pulses.

Trends in C═O Concentrations. On the basis of **Table 2**, we explored potential changes in the amount of types of C═O groups induced by milling and lignin extraction. The milling process involves depolymerization of the lignin polymer, mostly by cleavage of labile ether bonds. Another consequence of milling is that radical generation can lead to oxidation reactions, resulting in C═O groups (*38*). As milling proceeds, lower molecular weight lignin fragments are created, which can be solubilized in aqueous dioxane, becoming the MWL fraction. It is suspected that a large number of the oxidized structures are extracted in the dioxane-soluble portion, resulting in an overrepresentation of C═O structures. Solid-state NMR can quantify the levels of naturally incorporated C═O structures versus those generated by milling.

The data in **Table 2** show that the nonprotonated C═O structures were higher in abundance than the aldehyde groups in all samples studied. The total C═O concentration was the lowest in the juvenile wood (0.10 per aromatic ring) and increased slightly in the mature wood (0.14 per aromatic ring). The contributions of aldehydes in the two intact woods were similar, whereas the nonprotonated C═O concentrations were clearly higher in the mature wood. The C═O concentrations in mature wood and Wiley milled wood agreed within the error margins, which indicated that no significant oxidation occurs during Wiley milling, a long accepted conclusion.

Intense further milling of Wiley milled wood to produce wood flour results not only in a reduction of particle size but also in structural changes in the cell wall components. In **Figure 6**, we observed increases in the total C═O concentrations above what was already present in the unmodified wood samples. The P-6 milling is a long, low-intensity rotary-milling process,

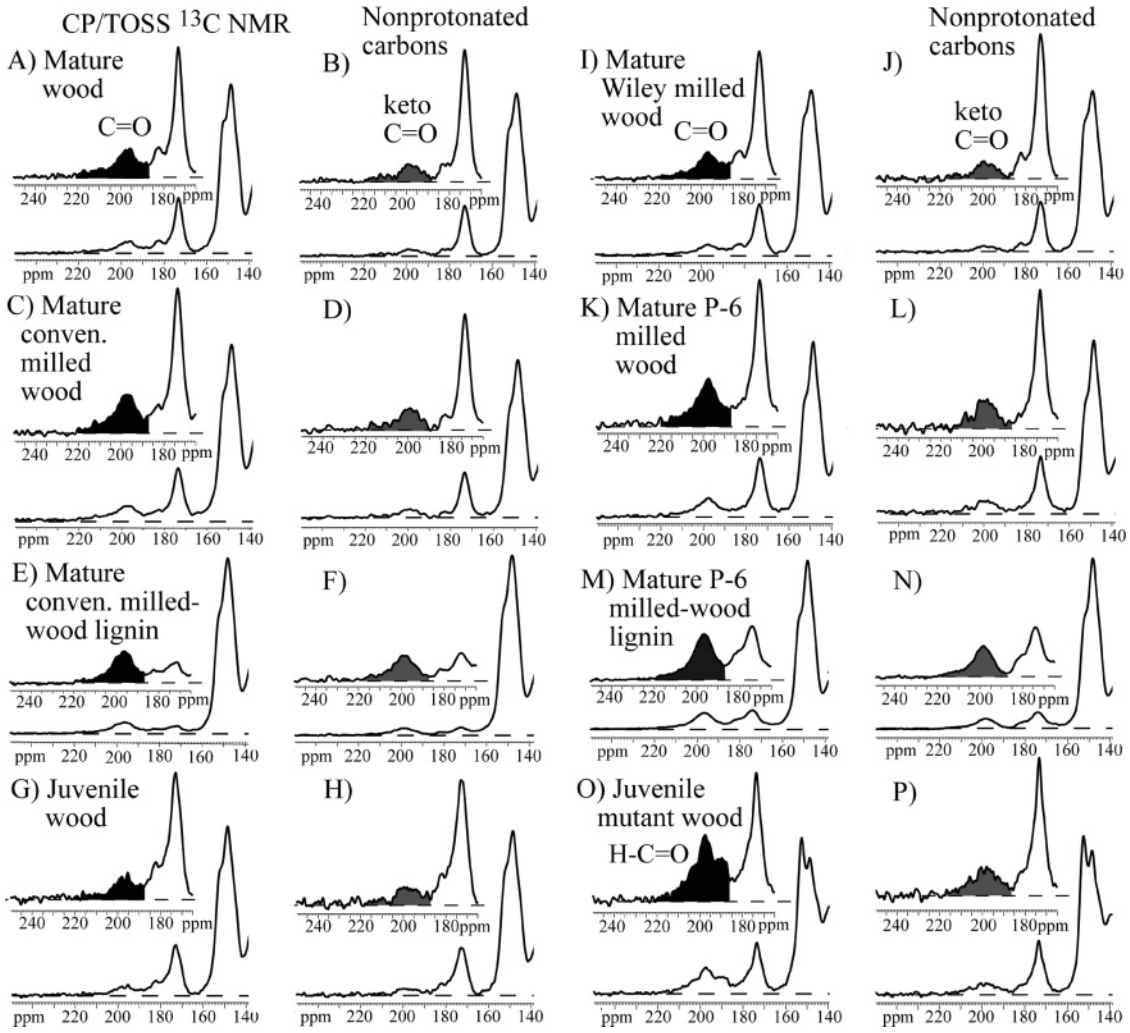

Figure 6. Aldehyde/ketone/aromatic C–O region (250–140 ppm) of the ^{13}C NMR spectra of **Figures 3** and **4**, scaled to equal height of the lignin aromatic C–O peak at 148 ppm. Above each spectrum, the region of 250–165 ppm is shown expanded vertically by a factor of 2.5 to make the small aldehyde and ketone bands more visible. Columns 1 and 3 were obtained without dipolar dephasing (all C═O, black area), columns 2 and 4 with dipolar dephasing (nonprotonated C═O, gray area). (**A**, **B**) Mature wood; (**C**, **D**) mature conventionally milled wood; (**E**, **F**) mature conventional MWL; (**G**, **H**) juvenile wood; (**I**, **J**) mature Wiley milled wood; (**K**, **L**) mature P-6 milled wood; (**M**, **N**) mature P-6 MWL; (**O**, **P**) juvenile mutant wood (homozygous CAD-deficient wood).

whereas the conventional milling process involves a much shorter but higher energy vibratory-milling process. The total C═O concentrations in the milled wood fractions (**Table 2**) increased with milling time (Wiley milling < conventional milling < P-6 milling), indicating that short, high-energy milling is better than a long milling process. The total C═O content increased 60% in the P-6 milled wood prepared from the Wiley wood meal from 0.15 to 0.24 per aromatic ring, but increased only ~25% in the conventionally milled wood, to 0.20 per aromatic ring.

The MWL fractions were similar in total C═O content per aromatic ring to the two milled-wood preparations from which they were extracted, although the content in the conventional MWL was slightly reduced. These results indicated that the dioxane extraction does not provide a MWL substantially enriched in oxidized material. It appears that end groups in the lower molecular weight fraction are not overly susceptible to oxidation reactions and that oxidation occurs throughout the lignin polymer.

Specific C═O-Bearing Structures. The relatively high ratio of keto to aldehyde groups (~0.10 to 0.03 structures per aromatic ring) in the mature wood and the Wiley milled wood is interesting to note. Nonprotonated C═O groups are likely to be at the α-position on the lignin side chain (i.e., conjugated carbonyls), and representative structures are likely to be β-aryl ethers with α-carbonyl constituents (**1**) and Ar−CO−CH_2−CH_2-OH (**2**) structures (**Figure 7**). The biosynthetic pathways for these types of structures are unclear, but these NMR data confirm that they do exist in unaltered wood and are not merely artifacts of the isolation process.

As mentioned, conjugated aldehyde structures were also present in unmodified wood, although to a lesser extent, 0.03−0.05 per aromatic ring in this study. Known aldehyde structures in wood are primarily coniferyl aldehyde (**3**) and vanillin (**4**). Finally, the recently proposed structure spirodienone (**5**) (*39*), which is a quinone methide trapped within a previously unreported β-1′ subunit, may be represented by the small peak at 182−180 ppm.

Several of the lignin structures in **Figure 7** can be confirmed by spectral editing. **Figure 8A** shows the overall CP/TOSS spectrum of the mature conventional MWL. The qualitative match with the solution ^{13}C NMR spectrum of the same sample (*18*) is good, if one takes into account a ~6 ppm inhomogeneous line broadening in the solid state. Most solution NMR signals in this guaiacyl-based lignin typical of conifers have been assigned to specific structures (*18*), some of which are shown

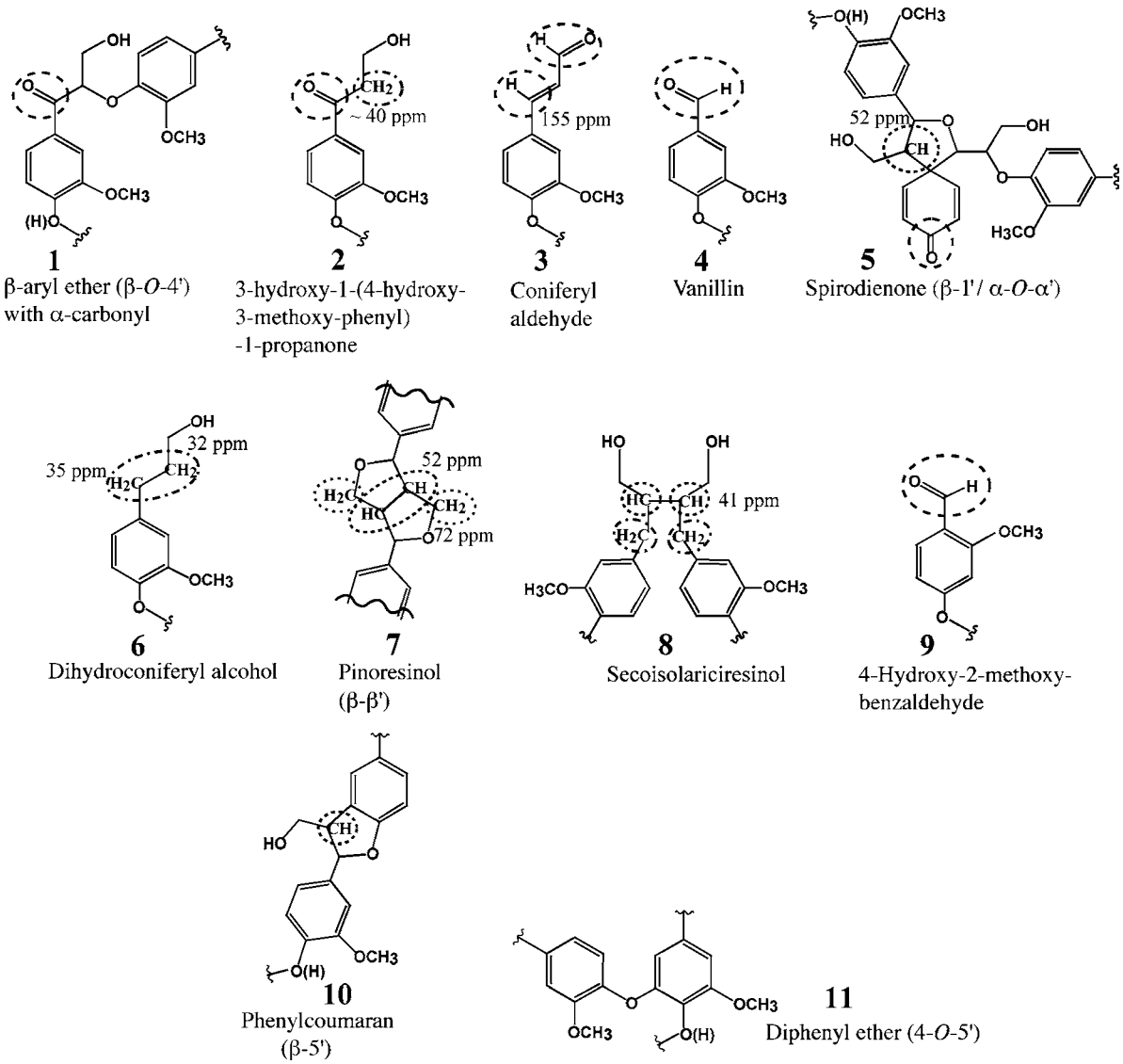

Figure 7. Structures containing keto, aldehyde, methine, and methylene groups identified by ^{13}C CP/TOSS and spectral-editing experiments. Groups specifically detectable in these solid-state NMR experiments have been highlighted.

Table 2. Estimated Number of C═O Carbons Resonating in the 220–187 ppm Range per Aromatic Ring[a]

	mature wood	Wiley milled wood	conventionally milled wood	MWL (conventional)	P-6 milled wood	P-6 MWL	juvenile wood	CAD-nl wood
all C═O	0.14	0.15	0.20	0.17	**0.24**	**0.25**	0.10	**0.30**
nonprotonated C═O	0.11	0.12	0.15	0.11	0.17	0.17	**0.06**	0.15
aldehydes	0.03	0.03	0.05	0.06	0.07	0.08	0.04	**0.15**

[a] The absolute uncertainty is on the order of ±20%, but the ratios of different values in the table are more reliable (±8%), allowing trends to be discerned.

in **Figure 7**. A feature in the solid-state NMR spectrum that is not obvious from the solution spectrum (in part due to the DMSO solvent peak near 39.5 ppm) was the significant fraction of nonpolar alkyl residues resonating at chemical shifts below 50 ppm. These accounted for $\sim^1/_{10}$ of all alkyl carbons in the two lignins studied. In spectra of CH_2 + CH groups (**Figure 8B**) and of protonated immobile alkyl sites (**Figure 8C**) these were also prominently visible. Spectral editing (**Figure 8D**,**E**) showed that they consist of a broad range of CH signals between 55 and 35 ppm, as well as a CH_2 band between 42 and 32 ppm. The latter can be assigned to $C-CH_2-C$ segments in structure **2** and, to a lesser extent, structures **6** and **8**. Whereas CH signals near 52 ppm have been assigned to CH not bonded to O, for example, in **5** and **7**, the only CH resonances previously reported below 50 ppm were from secoisolariciresinol (**8**), estimated by solution NMR to be ~0.02 per aromatic ring (*40*). The nonpolar alkyl bands were also present in Wiley milled wood (**Figure 8F**,**G**).

Other special protonated sites observed in these spectra at low intensities were the aldehydes near 193 ppm and the $=C_\alpha H$ vinyl sites of coniferyl aldehyde near 155 ppm. The latter seemed to be decreased in lignin compared to Wiley milled wood. Spectral editing also confirmed that near 72 ppm, $OC_\alpha H$ signals overlap with $C_\gamma H_2-O-C$ ethers found in $\beta-\beta'$ structures such as **7**.

NMR of Transgenic Whole Wood. NMR techniques suitable for elucidating specific structural information in solid wood samples can aid in the rapid assay of transgenic and bioengi-

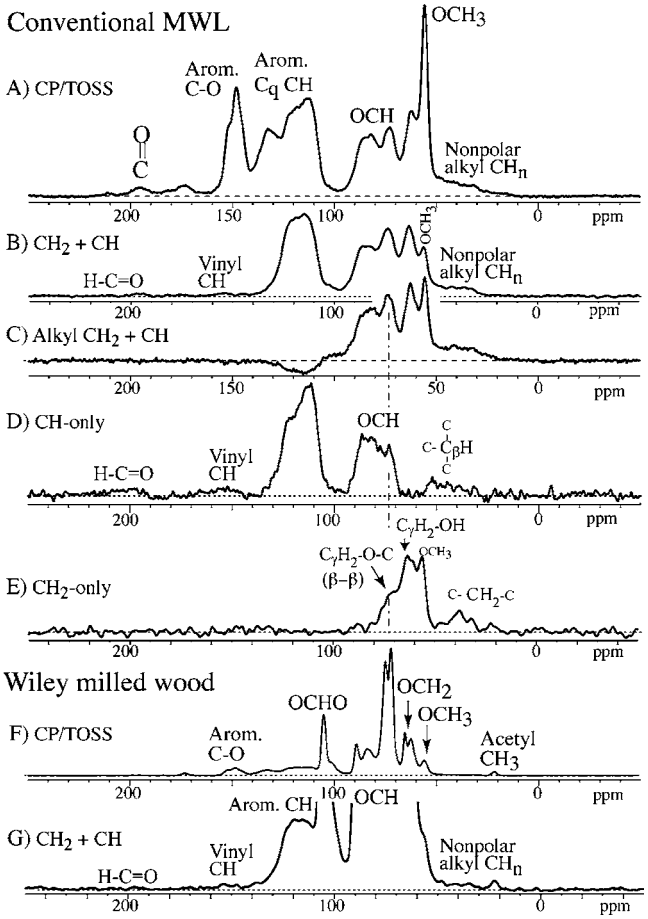

Figure 8. Spectral editing of (**A**–**E**) mature conventional MWL and (**F**, **G**) Wiley milled wood: (**A**) unselective CP/TOSS spectrum of MWL; (**B**) selection of immobile CH and CH_2 signals; (**C**) selection of immobile sp^3-hybridized CH_2 and CH carbons; (**D**) CH-only spectrum; (**E**) signals of immobile CH_2 groups; (**F**) unselective CP/TOSS spectrum of Wiley milled wood; (**G**) spectrum of immobile CH and CH_2 signals in Wiley milled wood, scaled so that the aromatic C–H band matches that in (**B**).

neered plants without isolation or modification of cell-wall components. As an example, we have studied whole wood from a 4-year-old loblolly pine that was 99% CAD-deficient. It was reported previously that these pines compensate for CAD deficiency by incorporating atypical subunits in the lignin biosynthetic pathway, most notably coniferyl aldehyde (**3**), vanillin (**4**), 4-hydroxy-2-methoxybenzaldehyde (**9**), and dihydroconiferyl alcohol (**6**) (*41*). Coniferyl aldehyde has a C_γ chemical shift centered at 196 ppm, whereas vanillin has a chemical shift in the range of 194−191 ppm. It was suggested from long-range C−H correlation NMR that 4-hydroxy-2-methoxybenzaldehyde (**IX**), a subunit previously undetected in lignins, was incorporated into the mutant wood (*41*). The juvenile CAD-deficient wood exhibited a shoulder centered at ∼190 ppm that disappeared in the dipolar dephasing spectra (**Figure 6O**,**P**), indicating an aldehyde. This observation supports the conclusion that 4-hydroxy-2-methoxybenzaldehyde is incorporated into the mutant wood. **Table 2** shows that the 4-year-old mutant wood contained 3 times the total C═O amount compared to the wild type, comprising 30% of the total monomeric input in the unmodified wood samples.

Figure 5 also shows dramatic differences in the aromatic region of the CAD-deficient wood. Typically, the C_4 carbon signal is a shoulder at 151 ppm on the more prominent peak of the C_3 carbon at 148 ppm, which is bonded to the methoxyl group. This can be seen in the juvenile wild-type sample in

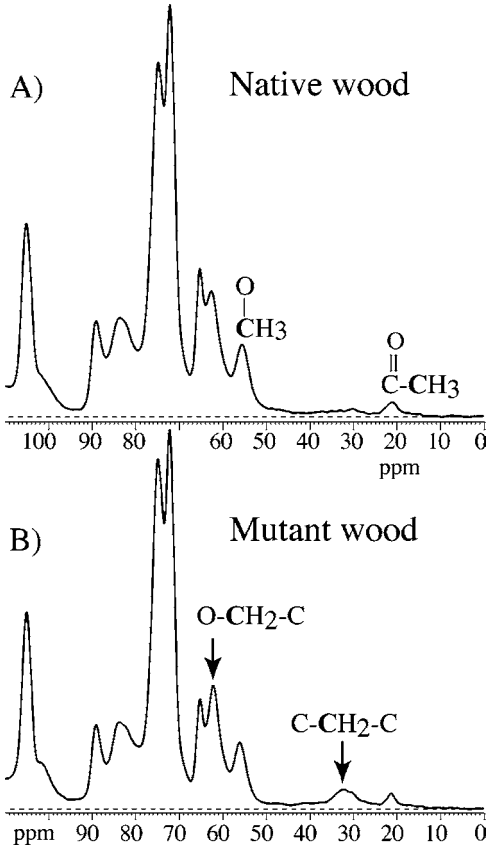

Figure 9. ^{13}C NMR CP/TOSS spectra of (**A**) juvenile wood (wild type) and (**B**) juvenile homozygous CAD-deficient wood (mutant wood) from loblolly pines. Signals characteristic of dihydroconiferyl alcohol in the mutant wood are labeled by arrows.

Figure 5A,**B**. In the mutant spectra, however, the signal at 151 ppm was more prominent than the C_3 peak at 148 ppm (**Figure 5C**,**D**). Nevertheless, the juvenile mutant appeared to have a similar or higher methoxyl content. The difference in the ratio of the peaks at 151 and 148 ppm can be explained at least in part by the incorporation of the 4-hydroxy-2-methoxybenzaldehyde subunit (**9**), the aromatic C−O (C_2 and C_4) signals of which are shifted downfield.

There was a prominent shoulder in both the ^{13}C and the dipolar dephased spectra at ∼140 ppm, indicating a nonprotonated aromatic carbon. This could be indicative of further structural changes in the lignin caused by incorporation of either the mentioned subunits or some other monomeric precursor. Ralph et al. (*41*) estimated that ∼15% of the subunits were either of the 4-hydroxy-2-methoxybenzaldehyde type or unknown. Of the known structural features in lignin, a peak in this area could possibly be indicative of an increase in β-5′ (**10**) or 4-*O*-5′ (**11**) structures, both of which have been reported to have resonances in the 144−142 ppm range in solution NMR.

Another striking characteristic in the solution-state NMR spectra of lignin extracted from homozygous CAD-deficient wood was a set of CH_2 resonances near 32 and 62 ppm, which have been assigned to the side chain of dihydroconiferyl alcohol **6** (*41*). **Figure 9** compares the alkyl-C region of unmodified mutant wood with that of the wild type. The 32 ppm resonance was clearly detected, and the 62 ppm signal could be deduced from the enhanced intensity in this spectral region. The area fraction of the peak of the two CH_2 groups near 32 ppm relative to the aromatic carbon signal was 14%. Taking into account the TOSS efficiency factor of ∼0.75 for the aromatic carbons, it was estimated that 0.3 dihydroconiferyl alcohol unit per

aromatic ring was incorporated into the CAD-nl wood, consistent with the 0.3 dihydroconiferyl alcohol unit per ring estimated from solution NMR of the extracted lignin (*41*).

In summary, we applied ^{13}C solid-state NMR to several wood and lignin samples. In particular, we quantified the amounts of aldehyde and protonated carbonyl structures in intact wood, proving that some are biosynthetically incorporated. There was no significant difference in the total aldehyde and ketone concentrations between mature wood and Wiley milled wood. However, total C═O fractions were increased by longer milling, without a strong effect of the intensity of milling. Consistent with higher total C═O concentrations in P-6 milled wood versus conventionally milled wood, there were more total C═O groups in P-6 MWL than in conventionally milled wood. The aldehyde and C−CH_2−C signals in the lignin of 99% CAD-deficient mutant wood were detected and estimated for the first time in the unprocessed wood, proving that they are biosynthetically incorporated.

The results obtained here highlight that solid-state NMR is a valuable method for characterizing structural details in whole-wood samples. The experiments allow for nondestructive, routine assay of genetically engineered sample sets for variations in cell-wall structure. Additionally, application of spectral-editing techniques can provide a detailed assessment of lignin structure in samples exhibiting abnormalities.

LITERATURE CITED

(1) Sarkanen, K. V. Precursors and their polymerization. In *Lignins: Occurrence, Formation, Structure and Reactions*; Sarkanen, K. V., Ludwig, C. H., Eds.; Wiley-Interscience: New York, 1971; pp 95−163.

(2) Higuchi, T. Biosynthesis of lignin. In *Biosynthesis and Biodegradation of Wood Components*; Higuchi, T., Ed.; Academic Press: Orlando, FL, 1985; pp 141−160.

(3) Terashima, N.; Fukushima, K. Biogenesis and structure of macromolecular lignin in the cell wall of tree xylem as studied by microautoradiography. In *Plant Cell Wall Polymers, Biogenesis and Biodegradation*; Lewis, N. G., Paice, M. G., Eds.; American Chemical Society: Washington, DC, 1989; No. 399, pp 160−181.

(4) Terashima, N.; Fukushima, K.; He, L.-F.; Takabe, K. *Forage Cell Wall Structure and Digestibility*; American Society of Agronomy, Crop Science Society of America, and Soil Science Society of America: Madison, WI, 1993; pp 247−270.

(5) Sederoff, R. R.; Chang, H. M. Lignin biosynthesis. In *Wood Structure and Composition*; Lewin, M., Goldstein, I. S., Eds.; Dekker: New York, 1991; pp 263−286.

(6) Fengel, D. Ideas on the ultrastructural organization of the cell wall components. *J. Polym. Sci. C* **1971**, *36*, 383−392.

(7) Yamamoto, E.; Bokelman, G. H.; Lewis, N. G. Phenylpropanoid metabolism in cell walls. In *Plant Cell Wall Polymers, Biogenesis and Biodegradation*; Lewis, N. G., Paice, M. G., Eds.; American Chemical Society: Washington, DC, 1989; No. 399, pp 68−88.

(8) Ludemann, H.-D.; Nimz, H. H. ^{13}C-NMR spectra of lignins. 2. Beech and spruce Bjorkman lignin. *Makromol. Chem.* **1974**, *175*, 2409−2422.

(9) Bartuska, V. J.; Maciel, G. E.; Bolker, H. I.; Fleming, B. I. Structural studies of lignin isolation procedures by ^{13}C NMR. *Holzforschung* **1980**, *34*, 214−217.

(10) Nimz, H. H.; Robert, D.; Faix, O.; Nemr, M. Carbon-13 NMR spectra of lignins, 8. structural differences between lignins of hardwoods, softwoods, grasses, and compression wood. *Holzforschung* **1981**, *35*, 16−26.

(11) Nimz, H. H.; Tschirner, U.; Stahle, M.; Lehmann, R.; Schlosser, M. Carbon-13 NMR spectra of lignins, 10. comparison of structural units in spruce and beech lignin. *J. Wood Chem. Technol.* **1984**, *4*, 265−284.

(12) Landucci, L. L. Quantitative ^{13}C NMR characterization of lignin. *Holzforschung* **1985**, *39*, 355−359.

(13) Bardet, M.; Foray, M. F.; Robert, D. Use of the DEPT sequence to facilitate the ^{13}C NMR structural analysis of lignins. *Makromol. Chem.* **1985**, *186*, 1495−1504.

(14) Chen, C.-L.; Robert, D. Characterization of lignin by ^{1}H and ^{13}C NMR spectroscopy. In *Methods in Enzymology: Biomass, Part B Lignin, Pectin, and Chitin*; Wood, W. A., Kellogg, S. T., Eds.; Academic Press: San Diego, CA, 1988; pp 137−174.

(15) Robert, D. Carbon 13 nuclear magnetic resonance spectroscopy. In *Methods in Lignin Chemistry*; Lin, S. Y., Dence, C. W., Eds.; Springer-Verlag: Berlin, Germany, 1992; pp 250−273.

(16) Ralph, J.; Marita, J. M.; Ralph, S. A.; Hatfield, R. D.; Lu, F. C.; Ede, R. M.; Peng, J. P.; Quideau, S.; Helm, R. F.; Grabber, J. H.; Kim, H.; Jimenez-Monteon, G.; Zhang, Y.; Jung, H. J. G.; Landucci, L. L.; MacKay, J. J.; Sederoff, R. R.; Chapple, C.; Boudet, A.-M. Solution-state NMR of lignins. In *Advances in Lignocellulosics Characterization*; Argyropoulos, D. S., Ed.' TAPPI Press: Atlanta, GA, 1999; pp 55−108.

(17) Xia, Z.; Akim, L. G.; Argyropoulos, D. S. Quantitative ^{13}C NMR analysis of lignins with internal standards. *J. Agric. Food Chem.* **2001**, *49*, 3573−3578.

(18) Holtman, K. M.; Chang, H.-M.; Hasan, J.; Kadla, J. F. Quantitative ^{13}C NMR characterization of milled wood lignins isolated by different milling techniques. *J. Wood Chem. Technol.* **2006**, *26*, 21−34.

(19) Kilpelainen, I.; Sipila, J.; Brunow, G.; Lundquist, K.; Ede, R. M. Application of 2D NMR spectroscopy to wood lignin structure determination and identification of some minor structural units of hardwood and softwood lignins. *J. Agric. Food Chem.* **1994**, *42*, 2790−2794.

(20) Lai, Y. Z.; Sarkanen, K. V. Isolation and structural studies. In *Lignins: Occurrence, Formation, Structure and Reactions*; Sarkanen, K. V., Ludwig, C. H., Eds.; Wiley-Interscience: New York, 1971; pp 165−240.

(21) Ikeda, T.; Holtman, K.; Kadla, J. F.; Chang, H.-M.; Jameel, H. Studies on the effect of ball milling on lignin structure using a modified DFRC method. *J. Agric. Food Chem.* **2002**, *50*, 129−135.

(22) Hardell, H.-L.; Leary, G. J.; Stoll, M.; Westermark, U. Variations in lignin structure in defined morphological parts of spruce. *Svensk Papperstidn.* **1980**, *83*, 44−49.

(23) Lapierre, C.; Lallemand, J. Y.; Monties, B. Evidence of poplar lignin heterogeneity by combination of ^{13}C and ^{1}H NMR spectroscopy. *Holzforschung* **1982**, *36*, 275−282.

(24) Hori, K.; Meshitsuka, G. Structural heterogeneity of hardwood lignin: characteristics of end-wise lignin fraction. In *Lignin and Lignan Biosynthesis*; Lewis, N. G., Sarkanen, S., Eds.; ACS Symposium Series 697; American Chemical Society: Washington, DC, 1996; pp 173−185.

(25) Haw, J. F.; Maciel, G. E.; Schroeder, H. A. Carbon-13 nuclear magnetic resonance spectrometric study of wood and wood pulping with cross polarization and magic angle spinning. *Anal. Chem.* **1984**, *56*, 1323−1329.

(26) Maciel, G. E.; O'Donnell, D. J.; Ackerman, J. J. H. Hawkins, B. H.; Bartuska, V. J. A ^{13}C NMR study of four lignins in the solid and solution states. *Makromol. Chem.* **1981**, *182*, 2297−2304.

(27) Terashima, N.; Atalla, R. H.; Vanderhart, D. L. Solid state NMR spectroscopy of specifically ^{13}C-enriched lignin in wheat straw from coniferin. *Phytochemistry* **1997**, *46*, 863−870.

(28) Terashima, N.; Hafren, J.; Westermark, U.; VanderHart, D. L. Nondestructive analysis of lignin structures by NMR spectroscopy of specifically ^{13}C-enriched lignins Part 1. Solid state study of Ginkgo wood. *Holzforschung* **2002**, *56*, 43−50.

(29) Schmidt-Rohr, K.; Mao, J. D. Efficient CH-group selection and identification in C-13 solid-state NMR by dipolar DEPT and H-1 chemical-shift filtering. *J. Am. Chem. Soc.* **2002**, *124*, 13938−13948.

(30) Mao, J.-D.; Schmidt-Rohr, K. Methylene spectral editing in solid-state ^{13}C NMR by three-spin coherence selection. *J. Magn. Reson.* **2005**, *176*, 1−6.
(31) Mao, J.-D.; Schmidt-Rohr, K. Separation of aromatic-carbon ^{13}C NMR signals from di-oxygenated alkyl bands by a chemical-shift-anisotropy filter. *Solid State NMR* **2004**, *26*, 36−45.
(32) Wu, X.-L.; Burns, S. T.; Zilm, K. W. Spectral editing in CPMAS NMR. Generating subspectra based on proton multiplicities. *J. Magn. Reson. A* **1994**, *111*, 29−36.
(33) Opella, S. J.; Frey, M. H. Selection of nonprotonated carbon resonances in solid-state nuclear magnetic resonance. *J. Am. Chem. Soc.* **1979**, *101*, 5854−5856.
(34) Schmidt-Rohr, K.; Spiess, H. W. *Multidimensional Solid-State NMR and Polymers*; Academic Press: London, U.K., 1994.
(35) deAzevedo, E. R.; Hu, W.-G.; Bonagamba, T. J.; Schmidt-Rohr, K. Principles of centerband-only detection of exchange in solid state NMR, and extensions to four-time CODEX. *J. Chem. Phys.* **2000**, *112*, 8988−9001.
(36) Gil, A. M.; Neto, C. P. Solid-state NMR studies of wood and other lignocellulosic materials. *Annu. Rep. NMR Spectrosc.* **1999**, *37*, 75−117.
(37) Yokoyama, T.; Kadla, J. F.; Chang, H.-M. Microanalytical method for the characterization of fiber components and morphology of woody plants. *J. Agric. Food Chem.* **2002**, *50*, 1040−1044.
(38) Hon, D. N. S.; Srinivasan, K. S. V. Mechanochemical process in cotton cellulose fiber. *J. Appl. Polym. Sci.* **1983**, *28*, 1−10.
(39) Zhang, L. M.; Gellerstedt, G. NMR observation of a new lignin structure, a spiro-dienone. *Chem. Commun.* **2001**, 2744−2745.
(40) Capanema, E. A.; Balakshin, M. Y.; Kadla, J. F. A comprehensive approach for quantitative lignin characterization by NMR spectroscopy. *J. Agric. Food Chem.* **2004**, *52*, 1850−1860.
(41) Ralph, J.; MacKay, J. J.; Hatfield, R. D.; O'Malley, D. M.; Whetten, R. W.; Sederoff, R. R. Abnormal lignin in a loblolly pine mutant. *Science* **1997**, *277*, 235−239.

Received for review July 31, 2006. Revised manuscript received October 26, 2006. Accepted October 26, 2006. This work was supported by the National Science Foundation under Grant CHE-0138117.

JF062199Q